Int. j. adv. multidisc. res. stud. 2022; 2(4):724-731

Received: 27-06-2022
Accepted: 07-08-2022

International Journal of Advanced Multidisciplinary Research and Studies

ISSN: 2583-049X

Integrated 1D and 2D geoelectric subsurface imaging around some distressed buildings within Ilara-Mokin Town

[1] ET Faleye, [2] MO Ajayi, [3] BK Ishola, [4] BJ Falana

[1, 2] Department of Physical and Chemical Sciences, Elizade University, Ilara-Mokin, Ondo State, Nigeria
[3] Department of Applied Geophysics, Federal University of Technology, Akure, Ondo State, Nigeria
[4] Department of Geology, Obafemi Awolowo University, Ile-Ife, Osun State, Nigeria

Corresponding Author: **ET Faleye**

Abstract

Integrated geophysical investigation using 1D and 2D electrical resistivity techniques were employed for post-foundation investigation around some distressed buildings in Ilara-Mokin, Ondo State, Nigeria. The study was carried out with the aim of characterizing subsoil materials and determining the probable cause(s) of foundation failure within the area. Five (5) traverses with varying lengths from 16 – 57 m were established. The Vertical Electrical Sounding (VES) using the Schlumberger array and combined Horizontal Profiling (HP)/Vertical Electrical Sounding (VES) using the dipole-dipole array techniques were adopted for this study. Qualitative interpretation was done by visual inspection of the pseudosections generated using the DIPRO™ software while VES data were interpreted through partial curve matching and later refined by computer iteration technique using Resist Version 1.0. The pseudosections revealed lithological layers interpreted as the topsoil, weathered layer, partly weathered/fractured basement and fresh basement rock. Though these layers were not clearly defined partly due to the inhomogeneous properties of the soil material. The average depth to bedrock was observed to be 5 m with possible fracture zones occurring along traverses 2 and 3. The 1D and 2D images delineated very low resistivity and water clay formation, due to the swampy environment around the study site. The study concluded that the building foundation failures are caused by the incompetent water saturated clayey materials underlying the foundation structures.

Keywords: Post-foundation, Engineering structure, Subsurface, HP/VES techniques

1. Introduction

Engineering structures encompass a broad spectrum of infrastructures, ranging from simple to complex ones. The term is generally used to describe every man-made structure that has its foundation on the earth's surface (ground). This includes buildings, but the term structure can also be used to refer to any assemblage designed to bear loads, even if it is not intended to be occupied by people. Common examples of engineering structures include bridges, dams, railways, roads, tunnels and buildings of varying sizes.

In recent time, the recurring cases of building collapses have generated great concerns at local, national and global scales. These incidences are due to uncertainties associated with the design and planning of such structures. Most reported incidents come with scores of losses of lives. Apart from non-compliance with building regulations and non-enforcement of building codes (Fagbenle and Oluwunmi, 2010) [6], undermining of pre- and post-construction investigations have been identified as principal causes of such failures.

The nonlinear behavior of the soil under stress, the difficulty of estimating soil properties in an undisturbed condition and the high spatial variability; all make it impossible to predict the exact behavior of soil in time and space. These difficulties call for the adoption of a factor of safety that ensures an adequate margin against unexpected deviation in the prediction performance in construction (Owobete, 2016) [15].

Construction professionals, often for reasons of cost and other consideration sometimes do not include pre/post-construction investigation involving geophysical techniques. Where such studies are done, the findings are often not taken into consideration in the design and construction phase. This omission usually results in a failed structure that can manifest as ground subsidence, major cracks, road failure, fractional settlement of structure (Olorunfemi *et al*., 2000) [13]. Exploratory holes for recovery of subsurface materials for identification and laboratory analyses are often given sole consideration by construction engineers. However, the use of geophysical methods is now adjudged to be indispensable in general foundation studies in providing subsurface information at reasonable cost, location of critical areas for test drilling and also elimination of less favorable sites (Ako, 1976; Faleye and Omosuyi, 2011; Ayolabi *et al.*, 2012; Oni and Olorunfemi, 2016) [3, 8, 4, 14].

The relevance of both pre- and post- construction investigation using engineering geophysical approach have been demonstrated and revealed the presence of fractures/faults, heterogeneous near-surface geo-materials, low competent geologic materials and uneven basement topography which may precipitate subsidence related failure and eventual collapse of the foundation of the building (Bayode *et al.*, 2012; Adelusi *et al.*, 2013; Nwokoma *et al.*, 2015; Fajana *et al.*, 2016; Aigbedion *et al.*, 2019) [5, 1, 12, 7, 2].

To ensure safety, success, and economy in the construction of engineering structures, it is necessary to have knowledge of the geophysical characteristics of the site concerned. Post-construction investigation often serves as integrity test tool of existing engineering structures; therefore, helps in monitoring and forestalling impending failures of engineering structures. Therefore, the usefulness of engineering geophysics to site investigations for civil engineering purposes cannot be undermined.

This study integrated 1D and 2D techniques of the electrical resistivity method to characterize the subsoil materials and determine the probable cause(s) of building foundation failure within the study area.

Location Description and Geologic Setting

The study area is located within Ilara-Mokin town, Ondo State. The area is bounded by Northings 812500 mN and 812580 mN and Eastings 732380 mE and 732520 mE using the Universal Traverse Mercator (UTM) Zone 31 (Fig 1). The climatic condition of the area follows the pattern of the southwestern Nigeria where the climate is influenced mainly by south west monsoon winds from the ocean and dry northwest wind from Sahara Desert. High temperature and high humidity also characterized the climate. There are two distinct seasons, the rainy and the dry seasons. The rainy season lasts for about seven months (April to October). The mean rainfall is about 1524 mm per year. The atmospheric temperature ranges between 28ºC and 31ºC. Humidity is relatively high during the wet season and low during the dry season with a mean annual relative humidity of about 80 percent (NIMET; 2007) [11]. Ilara-Mokin is underlain by rocks of the Precambrian Basement Complex of Southwestern Nigeria (Rahaman, 1988) [16]. The lithologic units identified in the area include granite, migmatised biotite-hornblende-gneiss, quartzite, with migmatite-gneiss constituting the predominant units around the study area (Fig 2).

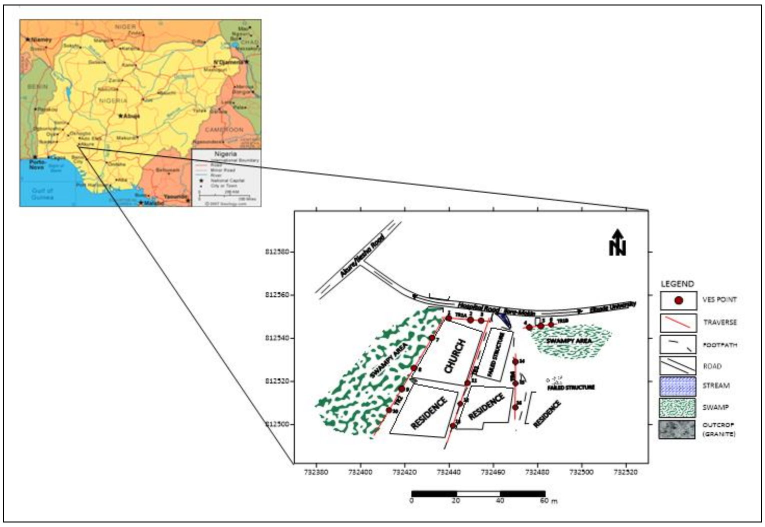

Fig 1: Base map of the study area, Top Left: Administrative map of Nigeria

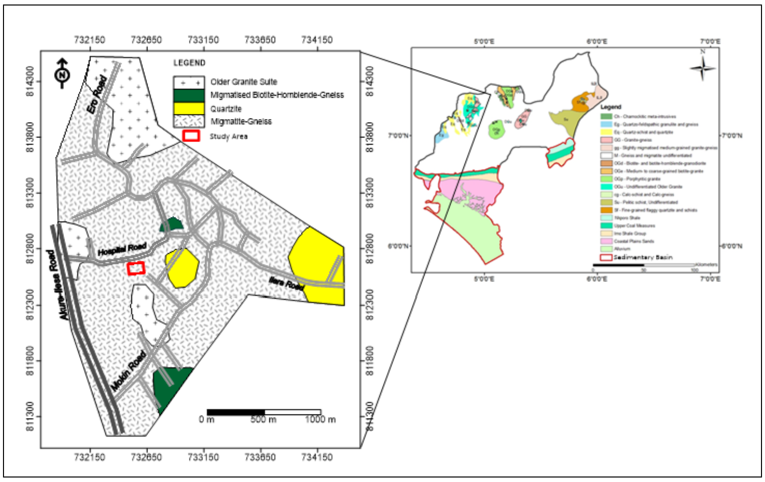

Fig 2: Geological map of the study area. Top Right Generalized Geologic Map of Ondo State (Adapted from Nigerian Geological Survey Agency, 1966)

2. Materials and methods

The combined horizontal profiling (HP) and Vertical Electrical Sounding (VES) involving the dipole-dipole array and Schlumberger array were adopted for the study. Five (5) dipole-dipole traverses for 2D subsurface imaging carried out were used to which constrain sixteen (16) depth soundings for subsurface 1D imaging. The 2D subsurface imaging utilized the dipole-dipole electrode configuration. Resistivity measurements were made at station interval of 1 m with an expansion factor (n), varying from 1 to 5. The dipole-dipole data were inverted into 2D subsurface images using the DIPRO software. The interpretation of the VES curve is both qualitative and quantitative. The qualitative interpretation involved visual inspection of the sounding curves while the quantitative interpretation utilized partial curve matching technique using 2-layer master curve which was later refined by computer iteration technique using Resist version 1.0 (Vander Velpen, 2004) [17] that is based upon an algorithm of Ghosh (1971) [9]. The partial curve matching can be regarded as preliminary interpretation of the field curves, which produced the starting geo-electric parameters needed for forward modeling. WinRESIST version 1.0 (Vander Velpen, 2004) [17] was used to perform the computer iterations. The resultant geo-electric parameters obtained from the iteration process were used to generate the geo-electric sections. The field equipment utilized for the study data acquisition are Ohmega resistivity meter and its accessories, global positioning system (GPS) and compass clinometer.

3. Results and discussion

2D Resistivity Structures

The pseudo-sections generated show the lateral and vertical variations of ground apparent resistivity values along established traverses. The 2D resistivity structure delineated four subsurface geo-electric layers; the topsoil, weathered layer, partly weathered/fractured basement and fresh basement rock.

Along Traverse 1A / Traverse 1B

An existing stream (Fig 1) resulted in the segmental parts of Traverse 1 (Traverses 1a and 1b). The resistivity distribution along the traverse (Fig 3a) revealed the complex and heterogeneous nature of the subsurface. A range of resistivity values diagnostic of conductive and fairly resistive layers were identified along this traverse. The resistivity values < 100 ohm-m and > 100 ohm-m (in reddish – purple colour band) represent the conductive and fairly resistive anomalous zones respectively. These zones are significantly distributed across the traverse, but are prominently delineated between stations 3 and 8, and between stations 9 and 14. The conspicuously visible blue colour band with resistivity values < 30 ohm-m is suspected to be clay body of high moisture content precipitated by the swampy nature of the study area. Fig 3b presents the 2D image underlying Traverse 1b. It is characterized by top soil with a generally low resistivity values < 50 ohm-m depicted by green - yellow colour range. The top soil is interpreted as clayey layer. Weathered layer and fresh basement were delineated having resistivity values ranging from 73-333 ohm-m and 360-766 ohm-m respectively. There is no evidence of discontinuities or shear zones along this traverse.

Along Traverse 2

Traverse 2 is located parallel to the swampy portion of the study area (Fig 1). About half of the traverse length is characterized by suspected clayey materials of high moisture content and very low resistivity values range; which may have resulted from the water-logged swamps around the area (Fig 4a). The resistivity range is < 100 ohm-m represented by blue – greenish colour band. The saturated zone could be responsible for subsidence observed at this part of the building. High resistivity values observed at the topsoil level are consequent of reinforcement materials constituting mainly shattered concrete blocks and sand laid down to limit the adverse effects of the seasonal flooding on the adjoining building. Weathered layer and fresh bedrock were delineated from station 20 to the end of the traverse. The undulating bedrock presents a surface expression of an outcrop between stations 25-27. Discontinuity at stations 24-32 is an indication of linear geologic fissure such as fracture, fault and shear zone. Similar features were observed between stations 34-36 but of a lesser magnitude.

Along Traverse 3

The 2D resistivity structure along Traverse 3 is presented as Fig 4b. From field observation, high compaction level was observed along the traverse which is parallel to and also cut-crossing a footpath. It is characterized by stable near-surface material with overlapping resistivity values generally > 50 ohm-m but < 300 ohm-m identified by blue – reddish colour band. Some spots of extremely low resistivity values (< 30 ohm-m) in blue colour band, delineated around stations 21–25 and 44–46 is diagnostic of pockets of clay. The similarities observed between Traverse 2 and Traverse 3 (Fig 4a and 4b); particularly the undulating basement characteristic shows a possible continuity of lithology and geologic features in the E-W direction.

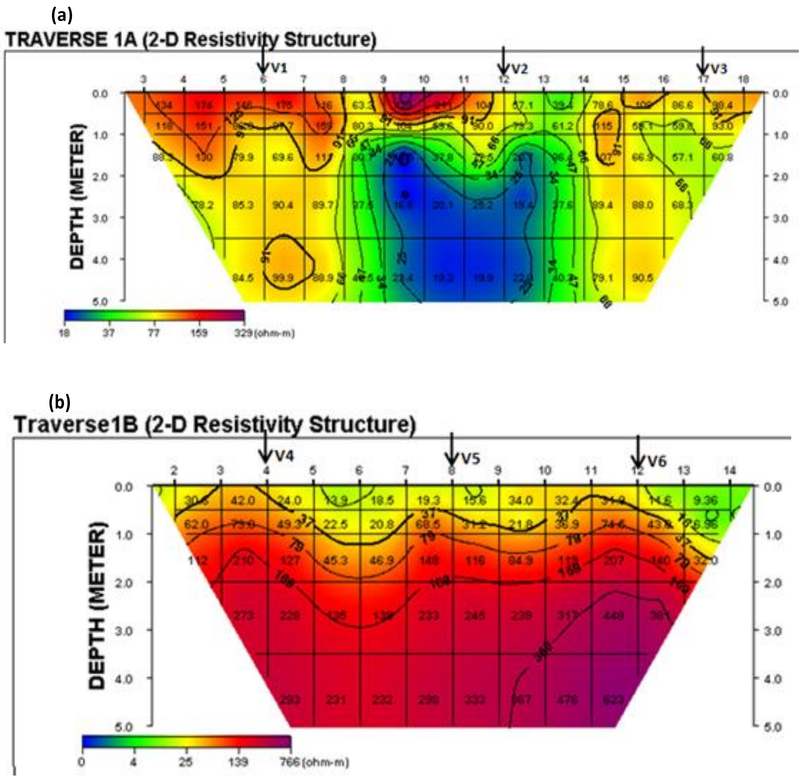

Fig 3a & b: 2D resistivity structure along Traverse 1a and Traverse 1b

Along Traverse 4

Similarly, as observed along Traverse 3, high degree of compaction was observed beneath 2D resistivity structure along Traverse 4 (Fig 4c). The topsoil lithology across the traverse constitutes sequence of weathered materials ranging from clay to clayey sand. These materials with resistivity values ranging from 70 ohm-m to 270 ohm-m (yellow – reddish colour bands) were delineated in most part of the traverse length as topsoil. The topsoil appears to be merged with weathered layer due to overlapping low resistivity values. The layer resistivity values of the weathered zone range are generally < 100 ohm-m and are characterized by green and yellow colour bands.

Vertical Electrical Sounding (VES) data

The VES summary of interpretation results is presented as the geo-electric parameters and geo-referenced data (Tables 1 & 2). The electrical soundings conducted were carried out in order to generate sounding profiles from which geo-electric sections were generated and thus provide subsurface information, which include layer resistivity and layer thickness. Typical depth sounding type curves obtained in the study area are A, H, AK, KH and HA (Fig 5).

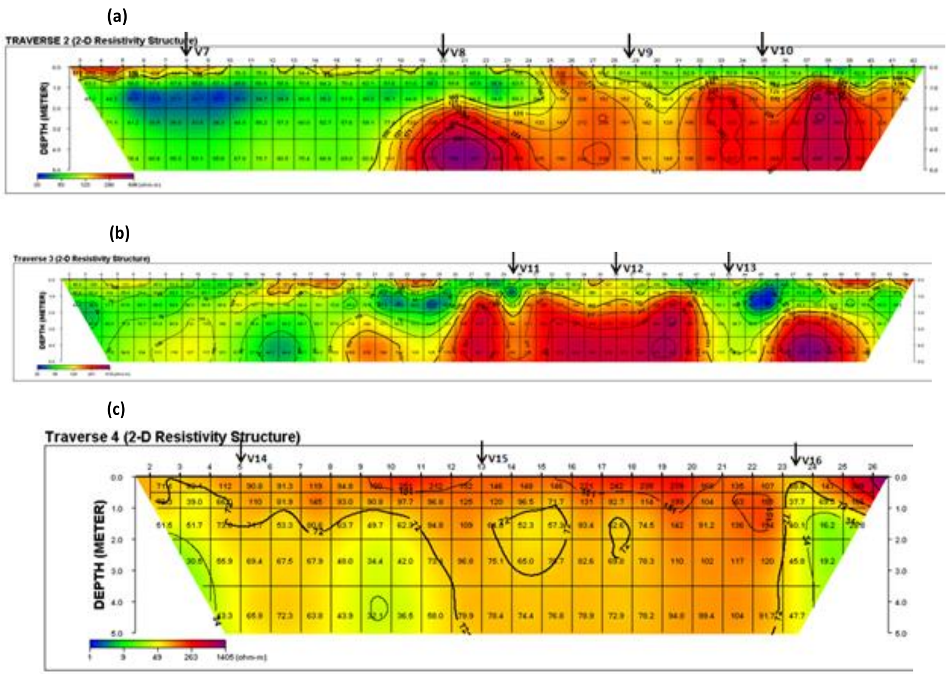

Fig 4 a-c: 2D resistivity structure along Traverses 2, 3 and 4

Table 1: Summary of subsurface geo-electric parameters

VES No	Resistivity (Ωm)				Thickness (m)				Type curve
	ρ_1	ρ_2	ρ_3	ρ_4	h_1	h_2	h_3	h_4	
1	35	94	36	10602	0.2	1.3	2.6	-	KH
2	13	588	30	329	0.1	0.2	2.1	-	KH
3	216	66	100000	-	0.3	6.7	-	-	H
4	46	75	1273	-	1.2	3.1	-	-	A
5	21	95	99576	-	1.4	4.7	-	-	A
6	20	112	186	-	1.3	5.9	-	-	A
7	85	26	1640	-	1.3	2.6	-	-	H
8	81	28	95305	-	0.8	1.7	-	-	H
9	86	26	1275	-	0.7	1.4	-	-	H
10	163	83	658	-	0.4	1.9	-	-	H
11	85	327	3108	-	1.4	4.7	-	-	A
12	154	600	2926	-	2.4	4.1	-	-	A
13	68	548	5410	167	1.2	2.4	3.2	-	AK
14	334	83	7187	-	0.4	1.6	-	-	H
15	471	60	1318	100000	0.3	1.0	1.3	-	HA
16	500	100	4400	-	0.3	3.0	-	-	H

Table 2: Field data coordinates

Traverse	VES No	Eastings	Northings	Elevation(m)
1a	1	732437	812553	330
1a	2	732442	812555	331
1a	3	732447	812553	331
1b	4	732458	812554	332
1b	5	732466	812554	330
1b	6	732470	812555	330
2	7	732432	812547	329
2	8	732427	812535	339
2	9	732422	812527	330
2	10	713245	812516	329
3	11	732441	812523	324
3	12	732445	812517	333
3	13	732442	812509	339
4	14	732460	812522	332
4	15	732461	812515	335
4	16	732460	812503	339

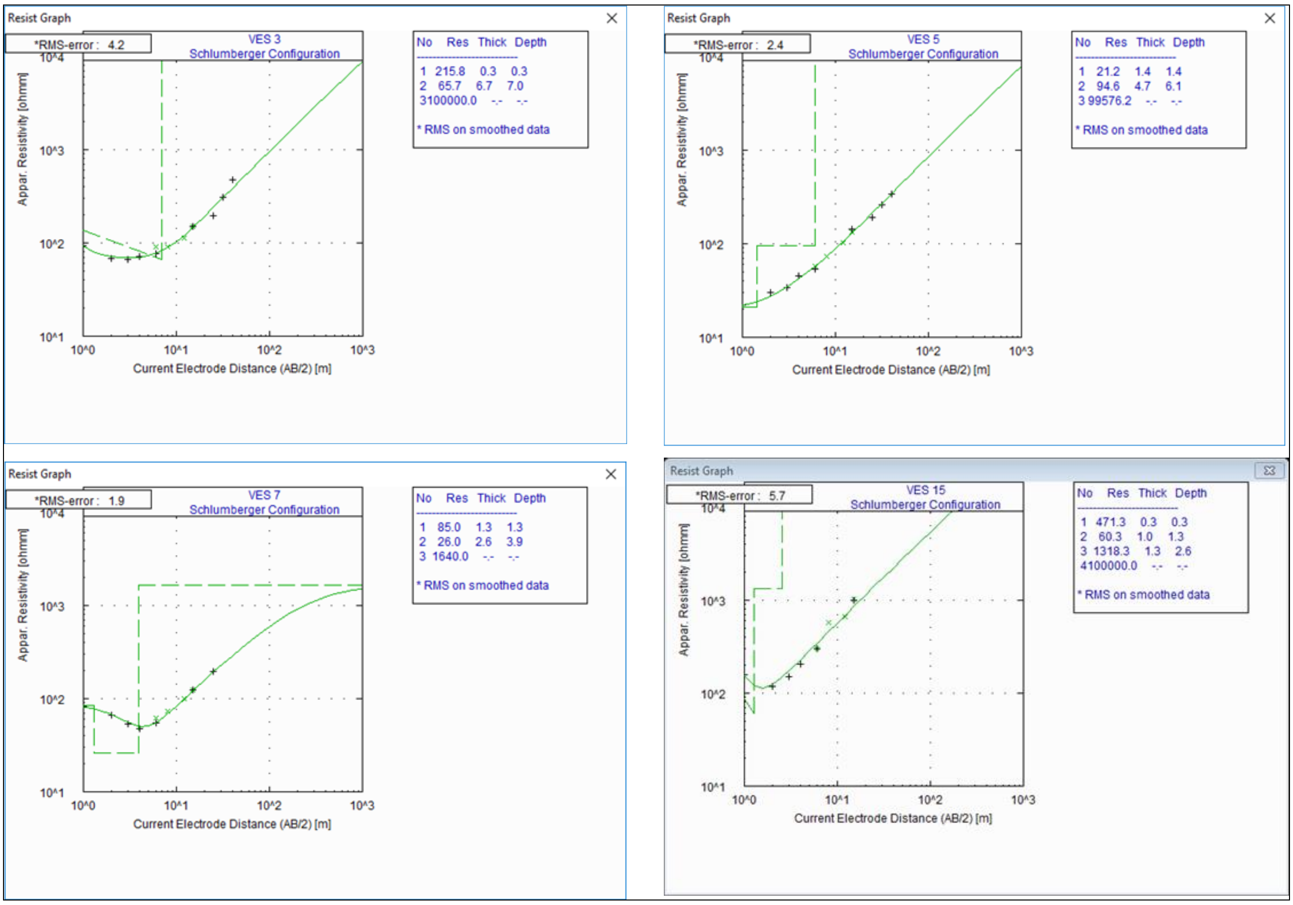

Fig 5: Typical H, A and HA -Type sounding curves from the Study area

Geo-electric Sections

The first order parameters obtained in form of layer thicknesses and resistivity values from the interpretation of the field curves were utilized in generating geo-electric sections. A total of five geo-electric sections were generated in the N-S and W-E directions. Typical geo-electric sections from the study delineated four (4) geologic layers (Fig 6 - 8).

Geo-electric Section along Traverse 1A

The section across Traverse 1a in W - E direction, constitutes VES stations 1, 2 and 3 (Fig 1). Four subsurface layers are delineated, the topsoil consisting clay/clayey sand, with a resistivity range of 13 Ωm – 588 Ωm and thickness range of 0.1 - 0.3 m. The weathered layer is composed of clayey formation with resistivity values ranging from 30 - 94 Ωm with lower resistivity values indicating zones of saturation; and thickness of about 7 m, partially weathered/fractured basement with resistivity value of 329 Ωm and thickness of 2.1 m was delineated beneath VES 2, while the depth to top of fresh basement occurs at depth range of 2.4 m – 7.0 m and resistivity values ranging from 10602 – 100000 Ωm. Significant correlation between the 2D resistivity structure and the geo-electric section was achieved.

Geo-electric Section along Traverse 1B

Traverse 1b cuts across VES 4, 5 and 6 in the W-E direction (Fig 1). The geo-electric section delineated three (3) layers including the topsoil, weathered layer and the fresh basement rock. The section depicts the topsoil interpreted as clay with a resistivity range of 20 – 46 Ωm and thickness range < 1.5 m. The weathered layer is interpreted as a sandy clay formation with resistivity values ranges from 75 –112 Ωm and thickness range of 3.1 – 5.9 m. The resistivity values range of 186 – 99576 Ωm of the last layer is diagnostic of the fresh basement. The 2D resistivity structure and the geo-electric section correlated well.

Geo-electric Section along Traverse 2

The geo-electric section along Traverse 2 in the N - S direction is presented as Fig 6a. The geo-electric section, comprising VES 7, 8, 9 and 10, delineates three (3) layers including the topsoil, weathered layer and the fresh basement rock. The section depicts the topsoil interpreted as sandy clay with a resistivity range of 80 – 163 Ωm and maximum thickness of about 1.3 m. The weathered layer is interpreted as a saturated clay formation. Resistivity values ranges from 26 – 83 Ωm. The last layer is the fresh basement occurring from depth interval of about 2.1 - 3.9 m and resistivity values ranging from 658 – 95305 Ωm. Fig 6b shows the correlation of the 2D resistivity structure with the geo-electric section.

Geo-electric Section along Traverse 3

Fig 7a presents the geo-electric section along Traverse 3, running in the N - S direction. The section comprises of VES stations 11, 12 and 13. Four subsurface layers are delineated, the topsoil consisting clay/sandy clay, with a resistivity range of 68 – 154 Ωm and thickness range of 1.2 – 2.4 m. The weathered layer is composed of sandy formation. Resistivity values ranges from 327 – 600 Ωm and thickness range of about 2.4 – 4.7 m; fractured basement to fresh basement occurs as the last layer with depth to top extent of 3.7 – 6.5 m and resistivity values ranging from 2926 – 5410 Ωm. Fig 7b shows the correlation of the 2D resistivity structure with the geo-electric section.

Geo-electric Section along Traverse 4

The geo-electric section along Traverse 4, combining VES 14, 15 and 16 is oriented in N-S direction (Fig 8a). It delineated four layers including the topsoil, weathered layer, partially weathered/fractured basement and the fresh basement rock. The section depicts thin compacted topsoil with resistivity values ranging from 333 – 500 Ωm and thickness < 0.5 m. The weathered layer has resistivity values between 60 and 100 Ωm with maximum thickness of 3.0 m, while the partially weathered/fractured basement is delineated beneath VES 15, with resistivity value of 1318 Ωm and thickness of 1.3 m. The resistivity values range of 4400 – 100000 Ωm is characteristics of the fresh basement. Depth to top of the fresh basement range between 1.9 m – 3.3 m. Fig 8b shows significant correlation of the 2D resistivity structure with the geo-electric section.

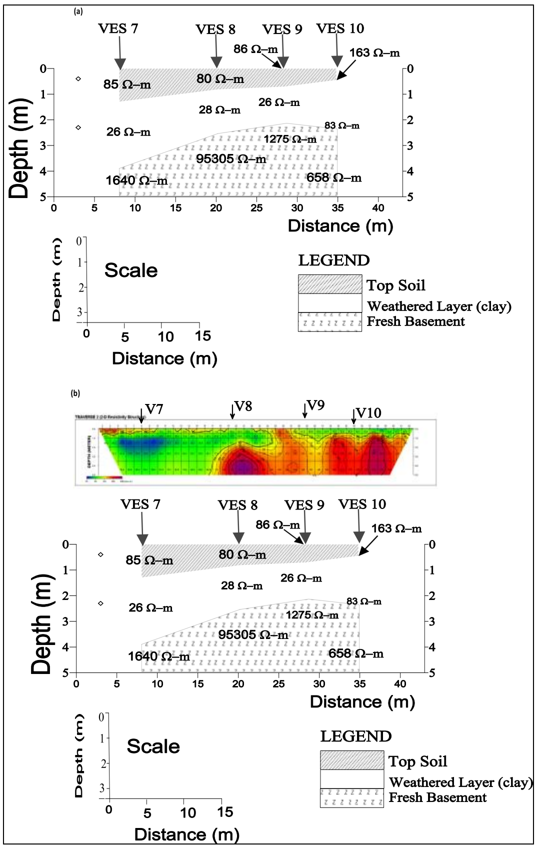

Fig 6: (a) Geo-electric section along Traverse 2 (b) Correlation along Traverse 2

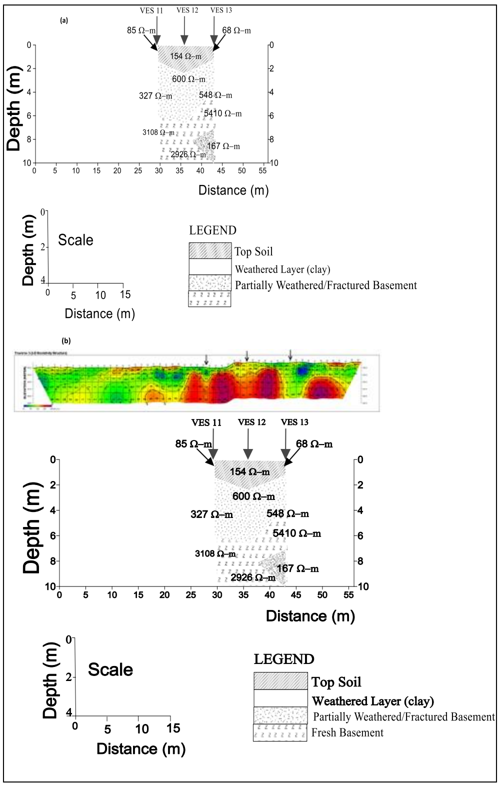

Fig 7: (a) Geo-electric section along Traverse 3 (b) Correlation along Traverse 3

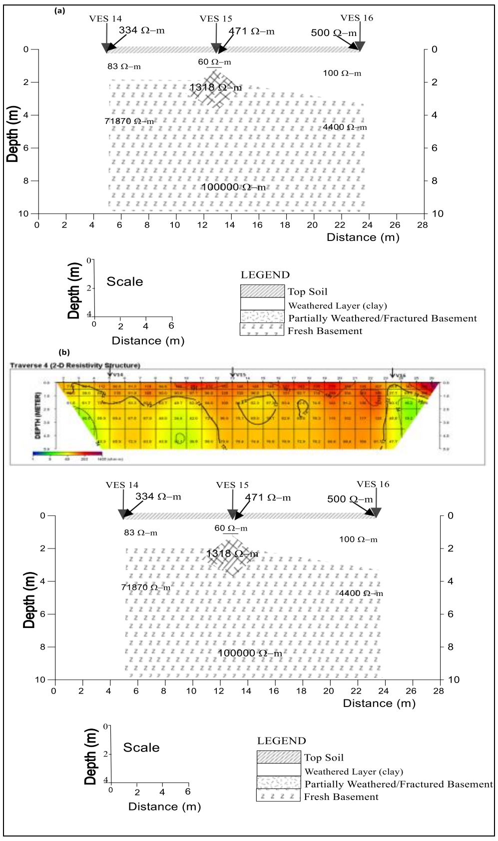

Fig 8: (a) Geo-electric section along Traverse 4 (b) Correlation along Traverse 4

4. Conclusion

From the VES survey, A, H, AK, KH and HA type curves were obtained. The H type is the most predominant, accounting for 43.75% while AK- and HA- type curves each account for 6.25%, representing the least occurrence. The inferred lithologies include; topsoil (clay/sandy clay), weathered/fractured bedrock and fresh bedrock as depicted on the generated geo-electric sections along the respective traverses. The topsoil (clay/clayey sand/sand) has resistivity and thickness values that vary from 13 to 588 Ωm and 0.1 to 2.4 m respectively. The second layer is the weathered layer (clay/sandy clay/sand) with resistivity values and thickness varying from 26 to 154 Ωm and 1.0 to 7.0 m respectively. The third layer is the (partially) weathered/fractured basement, with layer resistivity values that vary between 167 and 1318 Ωm and thickness that ranges from 1.3 to 2.1 m. The last layer is the fresh basement rock with high to very high resistivity values and depth to top varying from 2.1 to 7.0 m. The 2D resistivity structures imaged the topsoil, characteristics of conductive to fairly resistive materials (clay/clayey sand/sand). The topsoil (blue-green-yellow-reddish color), is with layer resistivity values that is > 30 Ωm and < 300 Ωm. The lower resistivity band typifies possibly water saturated conductive topsoil material, while the upper limit is the fairly compacted near-surface materials. The weathered layer (green-yellow-reddish color) has resistivity value > 70 Ωm and < 350 Ωm. The fresh basement (red-purple color) has significantly high resistivity value range. The topsoil and weathered layer depth range (< 3 m) which forms the foundation base within the study area, is predominantly composed of clay, sandy clay and sand formation, with significant variation in saturation and sand with variation in clay content; may precipitated the high rate of differential settlement being experienced by the distressed buildings. The study concluded that the foundation failures observed on the distressed buildings are precipitated by the non-competent (water saturated clayey materials) beneath the buildings' foundations.

5. References

1. Adelusi AO, Akinlalu AA, Nwachukwu AI. Integrated Geophysical investigation for post-construction of buildings around the school of science area, Federal University of Technology, Akure, Southwestern Nigeria: International Journal of Physical Sciences. 2013; 8(15):657-669.
2. Aigbedion I, Bawallah M, Ilugbo S, Osaigbovo AD, Diana EK, Ihewkwumere IC, *et al*. Geophysical investigation for Post Foundation studies at IKekogbe Primary school, Ekpoma, Edo State, Nigeria. American Journal of Environmental and Resources Economics. 2019; 4(2):73-83.
3. Ako BD. An integration of geophysical and geological data in damsite investigation: The case of Opa Dam. Jour. of Min. and Geology. 1976; 13(1):1-6.
4. Ayolabi EA, Folorunso AF, Jegede OE. An application of 2D electrical resistivity tomography in geotechnical investigations of foundation defects A case study. Journal of Geology and Mining Research. 2012; 3(12):142-151.
5. Bayode S, Omosuyi GO, Abdullai HI. Post foundation engineering geophysical investigation in part of Federal University of Technology, Akure, southwestern, Nigeria. Journal of Emerging Trends in Engineering and Applied Sciences (JETEAS). 2012; 3(1):203-201.
6. Fagbenle OI, Oluwunmi AO. Building failure and collapse in Nigeria: the influence of the informal sector. Journal of Sustainable Development. 2010; 3(4):268-276.
7. Fajana AO, Olaseeni OG, Bamidele OE, Olabode OP. Geophysical and geotechnical investigation for post foundation studies, Faculties of Social Sciences and Humanities, Federal University Oye-Ekiti: FUOYE Journal of Engineering and Technology. 2016; 1(1).
8. Faleye ET, Omosuyi GO. Geophysical and Geotechnical Characterisation of Foundation Beds at Kuchiyaku, Kuje Area, Abuja, (JETEAS). 2011; 2(5):864-870.
9. Gosh DP. The application of linear filter theory to the direct interpretation of geoelectrical resistivity sounding measurements. Geophysical Prospecting. 1971; 19(2):192-217. Doi: https//doi.org/10.1111/j.1365-2478.1971.tb00593.x.
10. Nigerian Geological Survey Agency. Compendium of geological maps of states in Nigeria, 1966.
11. Nigeria Meteorological Agency (NIMET). Daily weather Forecast on the Nigeria Television Authority. Nigerian Metrological Agency, Oshodi, Lagos, 2007.
12. Nwokoma EU, Chukwu GU, Amos-Uhegbu C. Geoelectrical investigation of soils as foundation materials in Umudike Area, southeastern Nigeria: Physical Science International Journal. 2015; 6(2):82-95.
13. Olorunfemi MO, Ojo JS, Sonuga F, Ajayi O, Oladapo MI. Geoelectrical and Electromagnetic Investigation of the Failed Koza and Nasarawa Earth Dams Around Katsina, Northern Nigeria. J. Mining Geol. 2000; 36(1):51-65.
14. Oni AG, Olorunfemi MO. Integrated geophysical investigation of the Igbara-Oke, Igbaraodo road pavement failure in Ondo/Ekiti State, Southwestern Nigeria. Ife Journal of Science. 2016; 18(1):119-131.
15. Owobete TM. Geoelectric sounding for pre-foundation investigation at SEMS phase 3 site, Federal University of Technology Akure, Nigeria. Unpublished, 2016.
16. Rahaman MA. Recent advances in the study of the basement complex of Nigeria. In: Geological Survey of Nigeria (ed) Precambrian Geol Nigeria, 1988, 11-43.
17. Vander Velpen, BPA. RESIST Version 10 M.Sc Research Project, ITC, Delf Netherland, 2004.